

# One Optimization on the Flight Trajectories of Re-entry Vehicle

Hiroyuki Takano\*, Kazuki Nakamura \*\*, Yoriaki Baba<sup>+</sup>

*Dept. of Aerospace Engineering  
National Defense Academy, Japan*

Keywords: Flight Dynamics, Optimal control, Re-entry

## Abstract

In this paper, we deal with some numerical analyses of a re-entry vehicle in a 2-dimensional plane as an optimal control problem. To reduce the dynamic load, the heat load and the oscillation in the trajectory, we researched the trajectories in which the load factor or the rate of flight path angle was minimized during reentry. In addition to that, taking advantage of the monotonous subarc method and the folded time-axis method, we tried to find the heat-less and load-less trajectory with combinations of some sectional functionals so that we can achieve more comfortability.

## Nomenclature

$a$	: speed of sound at sea level
$A$	: wing area (wetted)
$C_D$	: drag coefficient
$C_{D_0}$	: zero lift drag coefficient
$C_L$	: lift coefficient
$D$	: drag
$g$	: acceleration of gravity
$h$	: altitude
$I, J$	: functional
$K$	: induced drag coefficient
$L$	: Lift
$m$	: mass of re-entry vehicle
$Mach$	: Mach number ( $V/a$ )
$n$	: load factor
$q$	: heat rate
$t$	: time
$U_d$	: dummy control
$V$	: velocity
$W$	: weight of re-entry vehicle at sea level
$\gamma$	: flight path angle
$\theta$	: longitude
$\mu$	: gravity constant
$\nu$	: heat rate factor
$\rho$	: atmospheric density

$\tau$  : normalized time

## Subscripts

$( )_0$  : normalized initial value

$( )_1$  : normalized final value

$( )_f$  : final value

$( )_i$  : initial value

$( )_{max}$  : maximum value

## 1. Introduction

During the re-entry, the heat and the load are critical to the body because of several orders of density change with height and radical deceleration from semi-circular speed to less than Mach 10. In this period, radio communication is not available because of the Black Out. So it is necessary to provide the desirable trajectory for the mission in advance.

The purpose of our study is not only to seek the trajectory which reduces the dynamic load and heat transferred to the body but also to find more comfortable flight so that people can enjoy space travels without special training in the future. As a step for the comfortability, numerical calculations formulated in Sec. 3 with a method for the optimal control presented in Sec. 2 are attempted. We show the numerical results of load-minimum flight and gamma rate-minimum flight with heat constraint, and the trajectories with some sectional functionals in sec. 4. Some conclusions then are presented in Sec. 5.

## 2. The Optimal Control Problem

### 2.1 The General Problem

The purpose of this problem is to find the state  $\mathbf{x}(\tau)$ , control  $\mathbf{u}(\tau)$ , and the parameter  $\boldsymbol{\pi}$  so that the functional

$$I = \int_0^1 f(\mathbf{x}, \mathbf{u}, \boldsymbol{\pi}, \tau) d\tau + [h(\mathbf{z}(0), \boldsymbol{\pi})]_0 + [g(\mathbf{x}(1), \boldsymbol{\pi})]_1 \quad (1)$$

\* Lecturer, NDA, Yokosuka, Japan, 239

\*\* Graduate Student, NDA, Yokosuka, Japan, 239

+ Professor, NDA, Yokosuka, Japan, 239

is minimized, which satisfies the differential constraints, i.e., the equations of motion,

$$\dot{x} - \varphi(x, u, \pi, \tau) = 0, \quad 0 \leq \tau \leq 1 \quad (2)$$

the non-differential constraints,

$$S(x, u, \pi, \tau) = 0, \quad 0 \leq \tau \leq 1 \quad (3)$$

and the boundary conditions,

$$y(0) = \text{given}, [\omega(z(0), \pi)]_0 = 0, [\psi(x, \pi)]_1 = 0 \\ \text{with } x(0)^T = \{y(0), z(0)\}^T, \quad (4)$$

where  $z(0)$  is unknown initial state variable.

Using variable Lagrange multipliers  $\lambda(\tau)$ ,  $\rho(\tau)$ , and constant multiplier  $\sigma$ ,  $\mu$ , equation(1) can be transformed into an augmented functional

$$J = \int_0^1 [f + \lambda^T(\dot{x} - \varphi) + \rho^T S] d\tau \\ + (h + \sigma^T \omega)_0 + (g + \mu^T \psi)_1 \\ = \int_0^1 (-\dot{\lambda}^T x + f - \lambda^T \varphi + \rho^T S) d\tau \\ + (-\lambda^T x + h + \sigma^T \omega)_0 + (\lambda^T x + g + \mu^T \psi)_1. \quad (5)$$

From the calculus of variations or the optimal control theory, functions  $x(\tau)$ ,  $u(\tau)$ ,  $\pi$  and multipliers  $\lambda(\tau)$ ,  $\rho(\tau)$ ,  $\sigma$  and  $\mu$  must satisfy following optimality conditions.

$$\dot{\lambda} - f_x + \lambda^T \varphi_x - \rho^T S_x = 0, \quad 0 \leq \tau \leq 1, \quad (6)$$

$$f_u - \lambda^T \varphi_u + \rho^T S_u = 0, \quad 0 \leq \tau \leq 1, \quad (7)$$

$$\int_0^1 (f_x - \lambda^T \varphi_x + \rho^T S_x) d\tau \\ + (h_x + \sigma^T \omega_x)_0 + (g_x + \mu^T \psi_x)_1 = 0 \quad (8)$$

$$(-\zeta + h_x + \sigma^T \omega_x)_0 = 0 \quad (9)$$

$$(\lambda^T + g_x + \mu^T \psi_x)_1 = 0 \quad (10)$$

where  $\zeta(\tau)$  is the component of  $\lambda(\tau)$  associated with  $z(\tau)$ .

## 2.2 State Variable Constraints

Generally speaking, it is difficult to solve optimal control problems with state variable constraints

$$S = S(x, \tau) = 0 \quad (11)$$

instead of eq.(3). To solve eqs.(2)-(4) and eqs.(6)-(10) as a two-point boundary value problem, we must solve eqs.(3) and (7) for  $u$  and  $\rho$  to substitute them into eqs.(2) and (6), however, because of the lack of controls in eq.(11), we cannot solve them.

As the techniques to cope with the problem mentioned above, we used the folded time-axis method to solve multi-point boundary value problem as a two-point boundary value problem, and the monotonous subarc method not only keeps

state variables within the borderline but also holds  $\dot{S}$  either positive or negative with additional constraints,

$$S = \dot{S}(x, u, \pi, \tau) \pm U_d^2 = 0. \quad (12)$$

## 3. Formulation of the Re-entry

In this paper, the re-entry vehicle is represented as a point mass space shuttle-like space plane which re-enters the Earth's atmosphere in the vertical plane.

### 3.1 Equations of Motion

We consider a geocentric polar coordinate system illustrated in Fig.1 (In this figure, the Earth is non-rotating, spheric body). Therefore, equations of motion of the re-entry vehicle are as follows,

$$\dot{h} = V \sin \gamma \quad (13)$$

$$\dot{\theta} = \frac{V \cos \gamma}{R_E + h} \quad (14)$$

$$\dot{V} = -g \sin \gamma - \frac{\rho V^2 A C_D}{2m} \quad (15)$$

$$\dot{\gamma} = \frac{\rho V A C_L}{2m} - \left(\frac{g}{V} - \frac{V}{R_E + h}\right) \cos \gamma \quad (16)$$

where  $h$ ,  $\theta$ ,  $V$ ,  $\gamma$  are state variables, and  $\dot{h}$  denotes  $dh/dt$ . We employed  $C_L$  as a control variable, and the equality constraint is

$$S = C_L - C_{L_{\max}} \sin U_d = 0. \quad (17)$$

The atmospheric density is described as

$$\rho = \rho_0 e^{-\beta h} \quad (18)$$

and the acceleration due to gravity is

$$g = \frac{\mu}{(R_E + h)^2} \quad (19)$$

and the drag coefficient is

$$C_D = C_{D_0} + K C_L^2. \quad (20)$$

The constants for the equations are

$$A = 250 \text{m}^2, m = 89930 \text{kg}, C_{D_0} = 0.04, K = 1.2, R_E = 6378 \text{km}, \\ \mu = 0.398 \times 10^{-15} \text{m}^3/\text{s}^2, \rho_0 = 1.39 \text{kg/m}^3, \beta = 1/7162 \text{m}^{-1}$$

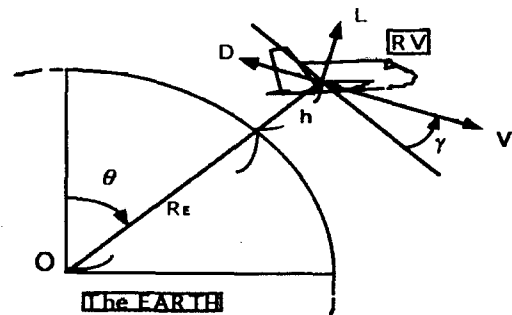


Fig.1 Coordinate System

### 3.2 Characteristics of

#### Approximate solutions

The results of calculation of fixed control  $C_L/C_D$  for  $\gamma_0 = -3\text{deg}$ . are shown in Fig.2. Here, load factor

$$n = \sqrt{\left(\frac{L}{W}\right)^2 + \left(\frac{D}{W}\right)^2} \quad (21)$$

and heat rate is normalized using  $V$  as

$$q = v \cdot \sqrt{\rho} V^3. \quad (22)$$

In Fig.2, we can easily recognize that the flat trajectory with smaller value of  $C_L/C_D$  does not descent to our final conditions:  $h_f = 50\text{km}$  and  $V_f = \text{Mach } 10$ , and if the  $C_L/C_D$  is larger, total heat becomes much amount and we cannot avoid oscillations in the trajectory.

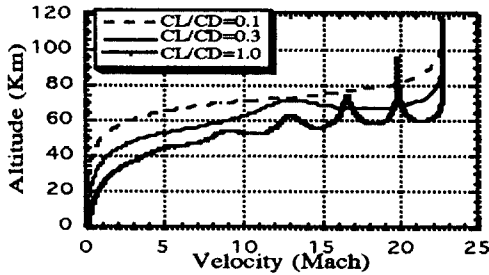


Fig. 2 h - V ( $C_L/C_D = \text{const.}$ )

## 4. Numerical Results

### 4.1 Trajectories with Heat Constraints

In this section, the total load-minimum flight and the total gamma rate-minimum flight with a heat constraint are considered. Using the monotonous subarc method, the heat constraint is imposed as

$$S = \frac{d}{dt}(v \cdot \sqrt{\rho} V^3) \pm U_d^2 = 0. \quad (23)$$

The functionals, to be minimized, are

$$I = \int_{t_i}^{t_f} \left\{ \left(\frac{L}{W}\right)^2 + \left(\frac{D}{W}\right)^2 \right\} dt, \quad (24)$$

and

$$I = \int_{t_i}^{t_f} (\dot{\gamma}^2) dt. \quad (25)$$

And the boundary conditions are

$$h_i = 120\text{km} \quad \theta_i = 0\text{deg} \quad \gamma_i = -3\text{deg}$$

and  $V_i$  is associated with  $\gamma_i$  by

$$V_i = \sqrt{\frac{2b(b-1)}{b^2 - \cos(\gamma_i)^2} \cdot \frac{\mu}{R_E + h_i}} \quad (26)$$

with  $b = \frac{R_E + h_c}{R_E + h_i}$   $h_c = 300\text{km}$ ,

$$h_f = 50\text{km} \quad V_f = \text{Mach } 10 \quad \theta_f: \text{free} \quad \gamma_f: \text{free}.$$

To solve this problem, SCGRA<sup>1)</sup> and MQA<sup>2)</sup> are applied.

The results of the total load-minimum flight are shown in Figs. 3-5 and the results for the gamma rate minimum flight are plotted in Figs. 6-8.

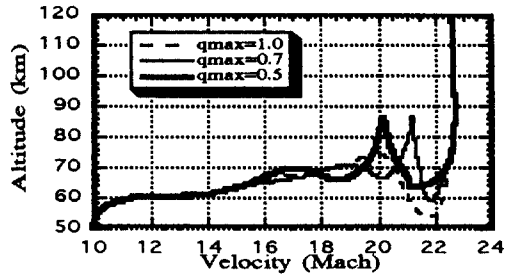


Fig. 3 h-V (n min)

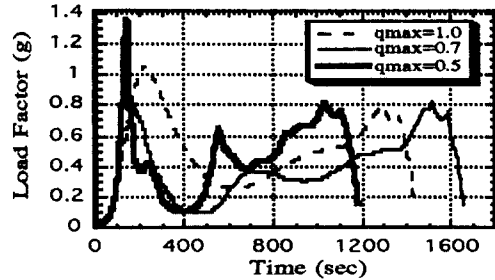


Fig. 4 Load Factor (n min)

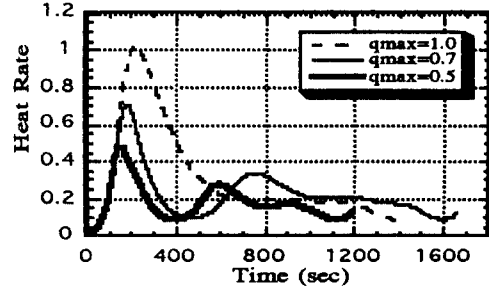


Fig. 5 Heat Rate (n min)

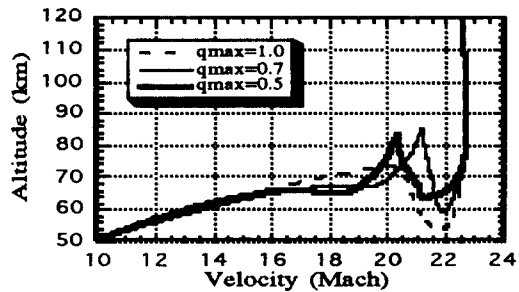


Fig. 6 h-V (gamma rate min)

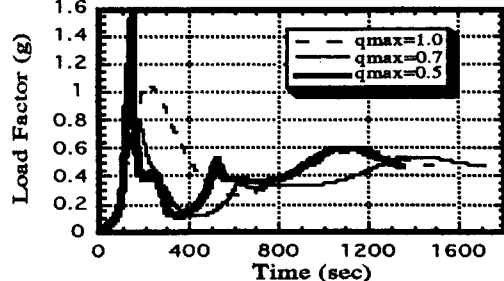


Fig. 7 Load Factor (gamma rate min)

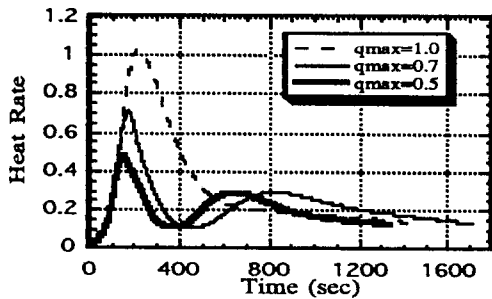


Fig. 8 Heat Rate (gamma rate min)

Figs 3-8 show that the smaller heat maximum is, the smaller the total heat is, and that the trajectory is flatter with the gamma rate minimum flight.

#### 4.2 An Application to the Folded Time-Axis Method

As an application of the folded time axis method, we divide the trajectory into three regimes of the time axis so that we can set a functional to each regime separately (see Fig. 9). For Regime-1, the rate of altitude  $\dot{h}$  is selected as functional, and for Regime-2 and 3, the total load or the total gamma rate is applied. The results are arranged in Figs 10-12.

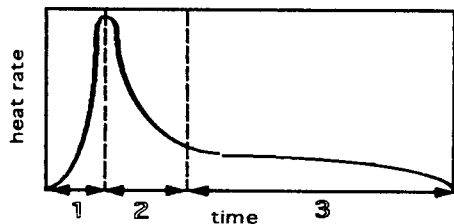


Fig. 9 The Subarcs

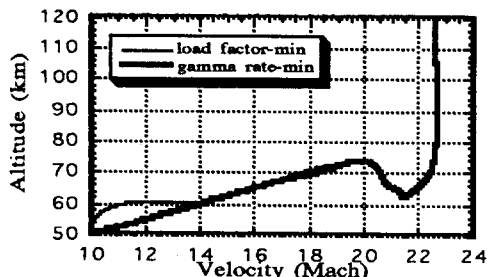


Fig. 10 Altitude vs Velocity

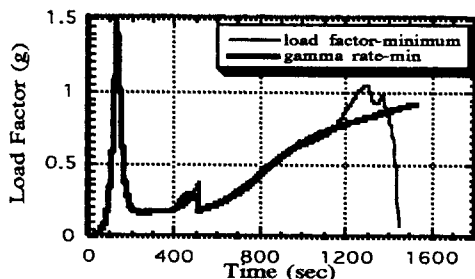


Fig. 11 Load Factor

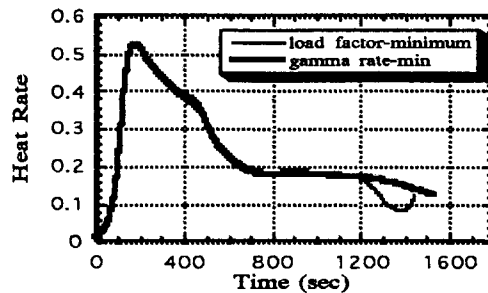


Fig. 12 Heat Rate

Figs. 10-12 show that the maximum heat rate is small while the change of the load factor and the heat rate is small. The trajectory is flatter with the gamma rate minimum flight.

#### 5. Conclusions

In order to reduce the heat and the load, it is fairly useful to impose functionals as the total load factor or the total gamma rate with the heat-maximum constraint. And with respect to the flatness on the trajectories, the total gamma rate-minimum flight is preferable. And the trial with the combined sectional functionals which are the altitude rate and the gamma rate is effective to flatten the trajectory with the small maximum heat rate.

In comparison with the results in section 4.1 and section 4.2, the approach with combined sectional functionals is more desirable with respect to the flatness of the trajectory and the change of the load factor and the heat rate. And it is important to impose the appropriate functionals because the results depend on the combination and the weight to each functional.

#### References

- 1) Wu, A.K., & Miele, A., *Optimal Control Applications & Methods*, 1-1, pp.69-88, 1980.
- 2) Gonzalez, S., & Rodriguez, S., *Journal of Optimization Theory and Applications*, 50-1, pp.109-128, 1986.
- 3) Takano, H., *Journal of the Japan Society for Aeronautical and Space Sciences*, 39-453, 1991.
- 4) Regan, Frank J., *Re-entry Vehicle dynamics*, 1984.
- 5) Kato, K., *Space Plane*, Tokyo Univ. Press, 1989.
- 6) Kato, K., *Optimal Control for Engineering*, Tokyo Univ. Press, 1988.